Supersymmetric enhancement of associated ZA^0 production at e^+e^- colliders

A.G. Akeroyd[1], A. Arhrib[2*], M. Capdequi Peyranère[3]

1: Korea Institute for Advanced Study, 207-43 Cheongryangri–dong, Dongdaemun–gu, Seoul 130–012, Korea

2: Physics Department, National Taiwan University 10764 Taipei, Taiwan, R.O.C

3: Laboratoire de Physique Mathématique et Théorique, CNRS-UMR 5825 Université Montpellier II, F–34095 Montpellier Cedex 5, France

Abstract

We study the associated production of the A^0 neutral CP–odd Higgs boson with a neutral gauge boson Z in high energy e^+e^- collisions at the one loop level. We present a detailed discussion for the total cross–section predicted in the context of the Minimal Supersymmetric Standard Model (MSSM) and make a comparison with the non–SUSY Two Higgs Doublet Model (THDM). We show that the MSSM cross-section may be enhanced compared to that for the THDM.

*On leave of absence from Department of Mathematics, FSTT, P.O.B416 Tangier, Morocco.

arXiv:hep-ph/0104243v3 29 May 2002

1. Introduction

The Standard Model (SM) of electroweak interactions [1] is in complete agreement with all precision experimental data (LEP, Tevatron, SLD). So far undiscovered is the SM Higgs boson (ϕ^0), which is the major goal of present and future colliders. Global SM fits [2] favour a relatively light ϕ^0, suggesting that it should be observed soon at forthcoming colliders. A light Higgs boson is also a feature of Supersymmetric (SUSY) theories, which are the most popular extensions of the SM. Since 1989 LEP has searched for ϕ^0 in the energy range 91 GeV $\leq \sqrt{s} \leq$ 208 GeV via the mechanism $e^+e^- \rightarrow Z^{(*)}\phi^0$. In the final run at energies around $\sqrt{s} = 208$ GeV two of the four experiments found excesses in the search for Higgs boson production [3] in association with a Z boson (Higgsstrahlung), while the other two presented improved lower limits on its mass [4] of $M_{\phi^0} > 109.7$ GeV and > 114.3 GeV.

LEP agreed that a further run with about 200 pb^{-1} per experiment at $\sqrt{s} = 208.2$ GeV would be enable the combined data from the four experiments to establish a 5σ discovery [5]. However the extended run was not approved and LEP was consequently shut down. The Higgs search will continue with Run II at the Tevatron [6] which has a chance of confirming the existence of the Higgs boson in the mass range hinted at by LEP ($M_{\phi^0} \approx 115$ GeV). This region is fairly problematic for the LHC [7] and would require several years searching for $\phi^0 \rightarrow \gamma\gamma$ decays in order to confirm such a light Higgs.

The still hypothetical Higgs sector of the Standard Model (SM) can be enlarged and some simple extensions such as the Minimal Supersymmetric Standard Model (MSSM) and Two Higgs Doublet Model (THDM) [8, 9] are under much intensive study. Both the THDM and MSSM introduce 2 Higgs doublets which break the electroweak symmetry [10]. From the 8 degrees of freedom initially present in the 2 Higgs doublets, 3 correspond to the masses of the longitudinal gauge bosons, leaving 5 degrees of freedom which manifest themselves as 5 physical Higgs particles (2 charged Higgs $H^\pm$, 2 CP–even H^0, h^0 and one CP–odd A^0). Aside from the charged Higgs sector, the neutral scalars of the THDM may possess a very different phenomenology to that of the SM Higgs. The discovery of a CP–odd Higgs boson or/and charged Higgs boson would be clear evidence of physics beyond the SM. Detection of a CP–even neutral Higgs with couplings differing significantly from those expected for ϕ^0 [11] would also provide evidence for physics beyond the SM. If the Higgsstrahlung cross–section is suppressed then the mass bound on such a Higgs boson is much weaker than the above bounds on M_{ϕ^0}.

Until now, no Higgs boson has been discovered, and from negative searches one can derive direct and indirect bounds on their masses. The combined null–searches from all four CERN LEP collaborations derive the lower limits $M_{H^\pm} \geq 77.3$ GeV and $M_A \geq 90$ GeV [5, 13] in the context of the MSSM.

CP-odd Higgs bosons can be produced at e^+e^- colliders [14] via $e^+e^- \rightarrow h^0A^0$ and $e^+e^- \rightarrow b\bar{b}A^0, t\bar{t}A^0$ [15],[16]. At future e^+e^- colliders the simplest way to produce CP–even Higgs scalars is in the Higgsstrahlung process $e^+e^- \rightarrow Z^* \rightarrow HZ$. The CP–odd A^0 possesses no tree-level coupling A^0ZZ, and the other tree–level diagrams for such a

process are proportional to the electron mass and consequently negligible [1]. The dominant contribution is therefore from higher order diagrams which will be mediated by both SM and non–SM particles. Therefore the rates are expected to be strongly model dependent.

Previous work on the loop induced production of Higgs bosons in association with gauge bosons (e.g. $e^+e^- \to A^0\gamma, H^\pm W^\mp$) can be found in [17, 18, 19] and references therein. Recently, associated production $\gamma\gamma \to ZH$, both for SM Higgs and MSSM Higgs, has been studied in [21]. In a previous paper [19] we studied the process $e^+e^- \to A^0Z$, in the context of the THDM. In this paper we extend the study to the case of the MSSM. The particle spectrum of the MSSM doubles that of the THDM, but the scalar sectors are equivalent up to some mass relations and differences in the couplings [8]. One would expect differences in the rates for the THDM and the MSSM, since in the latter there will be contributions from loops involving sparticles. If $e^+e^- \to Z^* \to A^0Z$ were sizeable it would provide an alternative way of producing A^0 at e^+e^- colliders, with a kinematical reach superior to that for the mechanism $e^+e^- \to Z^* \to A^0H^0$. Note that in the MSSM the kinematically favoured mechanism $e^+e^- \to Z^* \to A^0h^0$ is suppressed by the factor $\cos^2(\beta - \alpha)$ which is very small in the region $M_A \geq 200$ GeV. The study of the various production mechanisms of the CP–odd Higgs boson is well motivated since the discovery of such a particle would signify that the electroweak symmetry breaking is introduced by more that one Higgs doublet (ϕ^0 is CP–even).

Our work is organized as follows. In section 2 we outline our approach for evaluating the 1–loop rate for $e^+e^- \to A^0Z$ in the MSSM. In section 3 we present our numerical results and section 4 contains our conclusions.

2. One–Loop Corrections

In the limit of vanishing electron mass, the process $e^+e^- \to ZA^0$ posseses no tree–level contribution and is thus mediated by higher order diagrams. We have evaluated the one–loop amplitude in the 'tHooft–Feynman gauge. This amplitude contains ultraviolet divergences (UV) and we will use the dimensional regularization scheme [22] to deal with them.

The typical Feynman diagrams for the virtual corrections of order α^2 are drawn in Fig.1. These comprise:

(i) The fermionic contribution (s–channel) to the vertices γ-Z-A^0 and Z-Z-A^0: Fig.1.1 $\to$ 1.2 (+ crossed counterpart) and Fig.1.3

(ii) SUSY t–channel correction to the vertex $e^-e^{-*}A^0$: Fig.1.4, Fig.1.5 (+ crossed counterparts). This kind of vertex is non–vanishing in the limit of vanishing electron mass because one of the electrons is off–shell.

(iii) THDM box contributions, Fig. 1.6, and MSSM box contributions, Fig. 1.7 $\to$ 1.8, (+ crossed counterparts) and topology Fig. 1.9 and Fig. 1.10. Note that one–loop

---

[1]Note that at a muon collider [20], the tree–level diagrams cannot be discarded anymore and higher order diagrams would induce corrections to the tree-level rate.
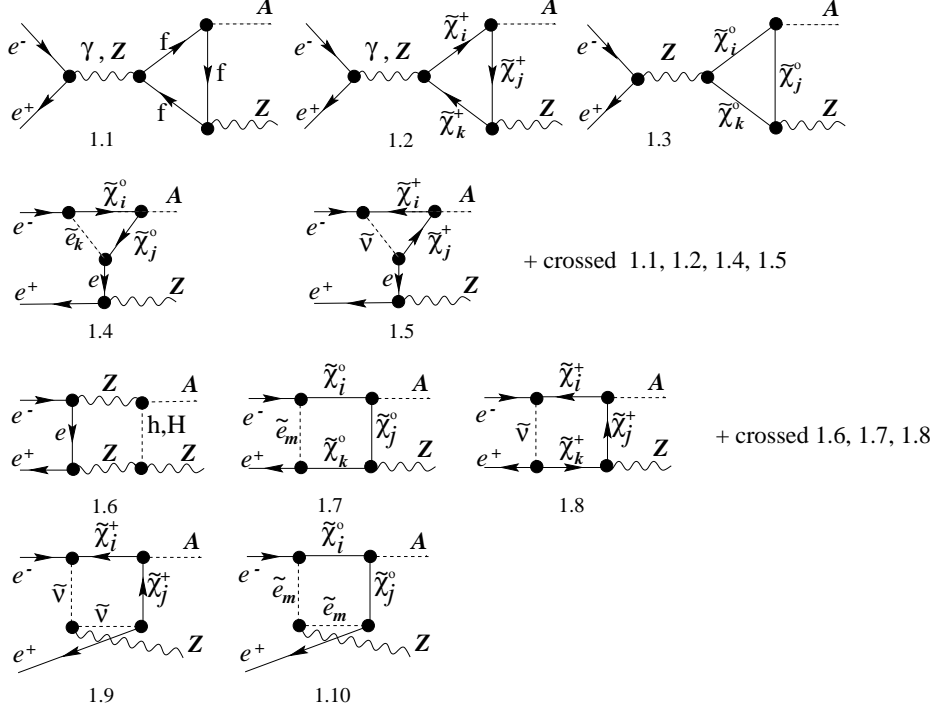
Figure 1: Generic Feynman diagrams (vertices and boxes) contributing to $e^+e^- \to ZA^0$ in the MSSM

contributions coming from initial state $e^+e^-H_0$, $e^+e^-h_0$ vertices also vanish in the limit $m_e \to 0$, since e^+ and e^- are both on–shell.

The t–channel vertex (Fig.1.5) and box diagrams Fig.1.8 and Fig.1.9 with exchange of charginos/sneutrinos contain vertices which violate fermion–number and we use Denner rules [23] to deal with them. All the Feynman diagrams are generated and computed using FeynArts and FeynCalc [24] packages. We also use the fortran FF–package [25] in the numerical analysis.

In the MSSM, the s–channel topology in (i) also receives contributions from sfermion triangular loops. However, the coupling of A^0 to a pair of sfermions satisfies the following relation: $(A^0 \tilde{f}_i \tilde{f}_j^*)_{i\neq j} = -(A^0 \tilde{f}_j \tilde{f}_i^*)_{i\neq j}$ and consequently the set of sfermions contributions to γ-Z-A^0 and Z-Z-A^0 vanishes.

Diagrams which involve Z-A^0 (resp Z-G^0) mixing in the s–channel self–energy and external lines vanish because the vertices γ-A^0-A^0 (resp γ-G^0-A^0) and Z-A^0-A^0 (resp Z-G^0-A^0) are absent. Z-A^0 mixing has to be considered in the t–channel, but owing to Lorentz invariance the Z-A^0 self–energy is proportional to CP odd momentum $p_{A^0}^\mu = (p_{e^+} + p_{e^-} - p_Z)^\mu$; then, since the vector boson Z is on–shell, the t–channel amplitude will be proportional to m_e and consequently vanishes. Note also that the tadpole diagrams have vanishing contributions. We stress in passing that, there are diagrams in the process $e^+e^- \to A^0 Z$ which do not contribute to $e^+e^- \to A^0\gamma$. These are diagrams which involve the couplings

4

$Z\chi^0\chi^0$ and $Z\tilde{\nu}\tilde{\nu}$, which would be absent if Z is replaced by γ.

At the one–loop order and in the limit of vanishing electron mass, the amplitude $\mathcal{M}^1$ fully projects onto six invariants, in a similar way as in the THDM [19], as follows:

$$\mathcal{M}^1 = \sum_{i=1}^{6} \mathcal{M}_i \mathcal{A}_i$$

where the invariants $\mathcal{A}_i$ are given by:

$$\mathcal{A}_1 = \bar{v}(p_{e^+}) \; \not{\epsilon}(p_Z)\frac{1+\gamma_5}{2}u(p_{e^-}) \qquad , \quad \mathcal{A}_2 = \bar{v}(p_{e^+}) \; \not{\epsilon}(p_Z)\frac{1-\gamma_5}{2}u(p_{e^-}) \qquad (2.1)$$

$$\mathcal{A}_3 = \bar{v}(p_{e^+}) \; \not{p}_Z\frac{1+\gamma_5}{2}u(p_{e^-})(p_{e^-}\epsilon(p_Z)) \quad , \quad \mathcal{A}_4 = \bar{v}(p_{e^+}) \; \not{p}_Z\frac{1-\gamma_5}{2}u(p_{e^-})(p_{e^-}\epsilon(p_Z))$$

$$\mathcal{A}_5 = \bar{v}(p_{e^+}) \; \not{p}_Z\frac{1+\gamma_5}{2}u(p_{e^-})(p_{e^+}\epsilon(p_Z)) \quad , \quad \mathcal{A}_6 = \bar{v}(p_{e^+}) \; \not{p}_Z\frac{1-\gamma_5}{2}u(p_{e^-})(p_{e^+}\epsilon(p_Z))$$

Here ϵ is the polarization vector of the gauge boson Z. Summing over the Z gauge boson polarizations, the squared amplitude may be written as:

$$\begin{aligned}
\sum_{ZPol} |\mathcal{M}^1|^2 &= 2s(|\mathcal{M}_1|^2 + |\mathcal{M}_2|^2) - \frac{(M_A^2 M_Z^2 - tu)}{4M_Z^2}\{4|\mathcal{M}_1|^2 + 4|\mathcal{M}_2|^2 + \\
&\quad 4(M_Z^2 - t)Re[\mathcal{M}_1\mathcal{M}_3^* + \mathcal{M}_2\mathcal{M}_4^*] + (M_Z^2 - t)^2[|\mathcal{M}_3|^2 + |\mathcal{M}_4|^2] \\
&\quad +4(M_Z^2 - u)Re[\mathcal{M}_1\mathcal{M}_5^* + \mathcal{M}_2\mathcal{M}_6^*] + (M_Z^2 - u)^2[|\mathcal{M}_5|^2 + |\mathcal{M}_6|^2] \\
&\quad -2(M_A^2 M_Z^2 + M_Z^2 s - tu)Re[\mathcal{M}_3\mathcal{M}_5^* + \mathcal{M}_4\mathcal{M}_6^*]\} \qquad (2.2)
\end{aligned}$$

The differential cross–section reads:

$$\frac{d\sigma}{d\Omega}(e^+e^- \to ZA^0) = \frac{1}{256\pi^2 s^2}\sqrt{(s - (M_A + M_Z)^2)(s - (M_A - M_Z)^2)} \sum_{ZPol} |\mathcal{M}^1|^2. \quad (2.3)$$

In the on–shell scheme defined in [26], it is found that there is no counter–term for the vertices Z-Z-A^0, Z-γ-A^0 and γ-γ-A^0. Consequently the one–loop vertices Z-Z-A^0, Z-γ-A^0 and γ-γ-A^0 have to be separately UV finite. It can be seen from the expression of the invariant $\mathcal{A}_i$ (eqs. 2.1) that the operators $\mathcal{A}_{1,2}$ are dimension 3 while operators $\mathcal{A}_{3,4,5,6}$ are dimension 5. One concludes that $\mathcal{M}_{3,4,5,6}$ have to be UV finite while $\mathcal{M}_{1,2}$ can potentially be UV divergent. We have checked numerically and analytically that the full set of invariants $\mathcal{M}_i$ are UV finite as required, and this feature will provide us with a good check of our calculation.

3. Numerical results and discussion

In this section we focus on the numerical analysis. We take the fine structure constant in the Thomson limit: $\alpha = 1/137.03598$.
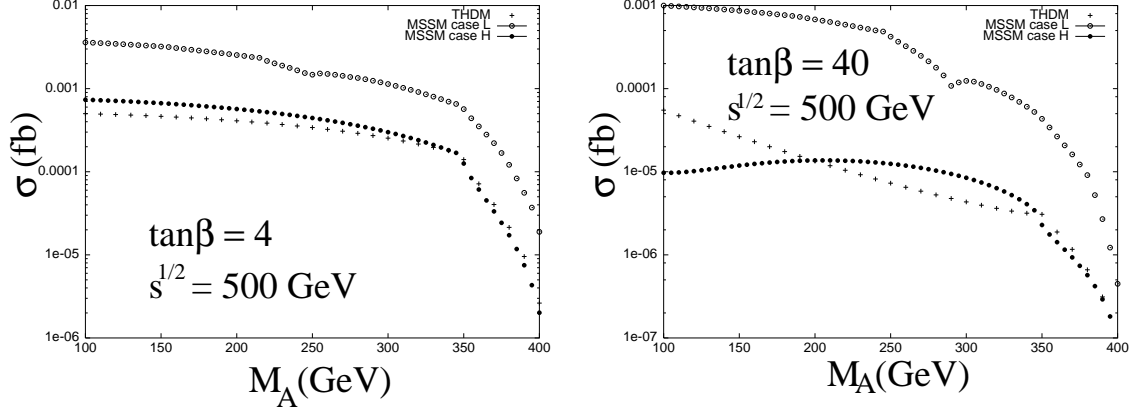
Figure 2: Total cross–section at 500 GeV centre of mass energy for $\tan\beta = 4$ (left) and $\tan\beta = 40$ (right)

The MSSM Higgs sector is parametrized by the mass of CP–odd M_A and $\tan\beta$ while the top quark mass and the associated squark masses enter through radiative corrections [27]. In our study we will include the leading corrections only, where the light Higgs mass is given by:

$$m_{h^0}^2 = \frac{1}{2}\left[m_{AZ}^2 - \sqrt{m_{AZ}^4 - 4m_A^2 m_Z^2 \cos^2(2\beta) - 4\epsilon\left(m_A^2 s_\beta^2 + m_Z^2 c_\beta^2\right)}\right]. \qquad (3.1)$$

with

$$m_{AZ}^2 = m_A^2 + m_Z^2 + \epsilon \qquad , \qquad \epsilon = \frac{3G_F}{\sqrt{2}\pi^2}\frac{m_t^4}{s_\beta^2}\log\left[\frac{m_{\tilde{t}}^2}{m_t^2}\right] \qquad (3.2)$$

The parameter $m_{\tilde{t}}^2 = m_{\tilde{t}_1}m_{\tilde{t}_2}$ denotes the average mass squared of the stop particles. A recent search for h^0 and A^0 excludes the region $0.5 < \tan\beta < 2.4$ [5], assuming maximal mixing in the stop sector. In light of this we limit ourselves to the case where $\tan\beta \geq 3$. Following the approach of [28] we assume a detection threshold of 0.1 fb for $e^+e^- \to A^0 Z$. This would give 50 events before experimental cuts for the expected luminosities of 500 fb^{-1}. In the THDM this criterion would require $\tan\beta \leq 0.3$, even for a light pseudoscalar [19].

The chargino/neutralino sector can be parametrized by the usual M_1, M_2 and μ. We limit ourselves to the case of $\mu > 0$ since $\mu < 0$ seems to be disfavoured by $b \to s\gamma$ constraint[2] and from recent measurements of the anomalous magnetic moment of the muon, $(g-2)_\mu$ [30]. We also use the SUGRA constraint $M_1 \approx M_2/2$ and take the left selectron, right selectron and sneutrino to be degenerate with a common mass $M_{\tilde{l}}$

We present our results for two specific cases: (i) Light SUSY case (case L), where all sleptons, charginos and neutralinos are relatively light with mass ≤ 200 GeV. (ii) Heavy SUSY case (case H) where all sleptons, charginos and neutralinos have mass ≥ 450 GeV.

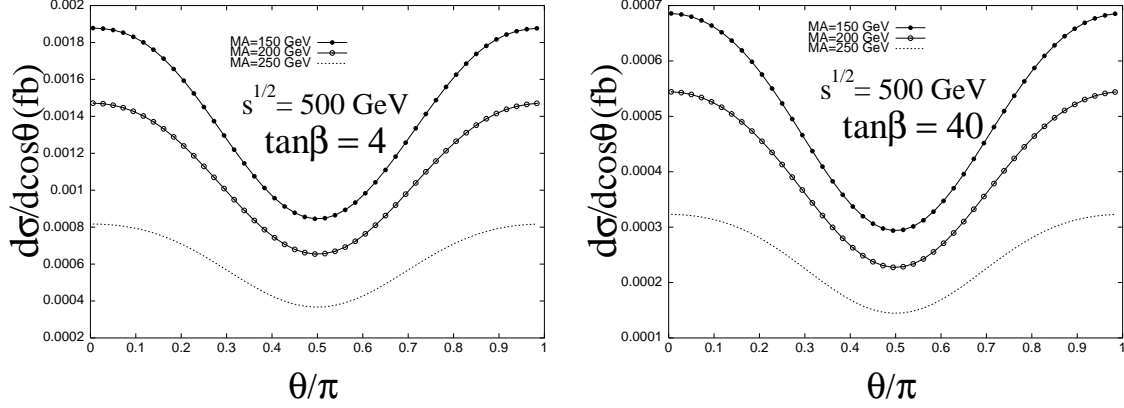[2]the chargino-stop contribution to $b \to s\gamma$ add constructively with the SM one for $\mu < 0$ [29].

Figure 3: Angular distribution $\frac{d\sigma}{d\cos\theta}$ (fb) for $e^+e^- \to ZA^0$, MSSM case L with $\tan\beta = 4$ (left) and $\tan\beta = 40$ (right)

- Case L: $M_2 = 220$, $\mu = 180$ and $M_{\tilde{l}} = 200$ GeV
- Case H: $M_2 = 500$, $\mu = 600$ and $M_{\tilde{l}} = 450$ GeV

We start by recalling that the THDM contribution to $e^+e^- \to A^0 Z$ [19] in the small $\tan\beta$ regime is enhanced by the top quark contribution, leading to significant cross–sections (about a few fb). In the large $\tan\beta$ regime the cross–section is suppressed and does not attain observable rates. In the MSSM we limit ourself to the case where $\tan\beta \geq 3$, and consequently the THDM contribution is suppressed to the order of ≈ 0.001 fb at $\sqrt{s} = 500$ GeV. Our aim is to see if the SUSY contribution can enhance the cross–section.

In Fig.2 we show the dependence of the total cross–section on the CP–odd Higgs mass M_A for $\sqrt{s} = 500$ GeV in the case where $\tan\beta = 4$ (Fig.3.a) and 40 (Fig.3.b). In both cases we show the MSSM contribution for case L and case H, as well as the THDM contribution. It can be seen that the light SUSY particle scenario (L) may enhance the total cross–section, which can reach ≈ 0.003 fb for $M_A \leq 300$ GeV and $\tan\beta = 4$, with smaller cross–sections for $\tan\beta = 40$. Note also that for $M_A \leq 300$ GeV the box contribution is an order of magnitude smaller than the vertex corrections in the MSSM case L, for both $\tan\beta = 4$ and 40. The kink observed in this figure close to $M_A \approx 2m_t$ is a threshold effect due to the opening of the decay $A^0 \to t\bar{t}$. One can also have other threshold effects which arise from charginos and neutralinos. Note that in the case L and for $\tan\beta = 4$ (resp 40) the mass of the light chargino is about 132.5 GeV (resp 146 GeV), and one can see a smooth threshold effect due to the opening of the channel $A^0 \to \tilde{\chi}_1^+ \tilde{\chi}_1^-$ for $M_A \approx 264$ GeV (resp $M_A \approx 290$ GeV). Due to the decoupling property of SUSY theory, the MSSM contributions in case H are very small and the total cross–section is close to the THDM one.

We illustrate in Fig.3 the angular distribution in the MSSM with light SUSY particles for $\sqrt{s} = 500$ GeV, $\tan\beta = 4$ (left curve) and $\tan\beta = 40$ (right curve). The shape of the graph is in agreement with that expected for a CP–odd scalar being produced by an
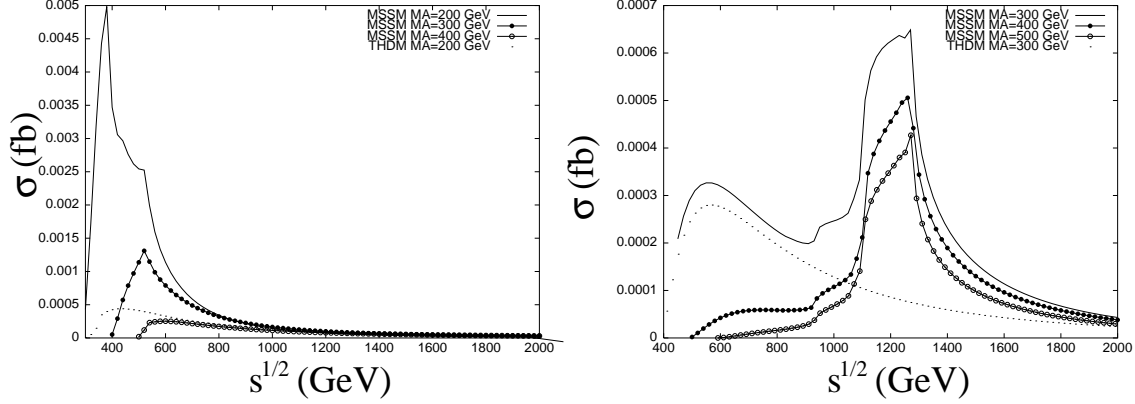
Figure 4: Total cross section σ (fb) for $e^+e^- \to ZA$, MSSM case L with $\tan\beta = 4$ (left) and MSSM case H ($\tan\beta = 4$ right)

effective ZZA^0 coupling [31].

We stress here that in both cases, the shape of the angular distribution originates from the vertex contribution, since the box contribution is rather small at $\sqrt{s} = 500$ GeV. In the case of heavy SUSY particles (MSSM case H) the total cross–section is suppressed which would render difficult any analysis of the angular distribution. The numerical value of $\frac{d\sigma}{d\cos\theta}$ lies in the range 0.0019-0.0009 fb (resp 0.0008-0.0004 fb) with $0 < \theta < \pi$ for $\tan\beta = 4$ and $M_A = 150$ GeV (resp $M_A = 250$ GeV). We note in passing that the corresponding values for the THDM with $\tan\beta \geq 3$ would also be very small.

It is interesting to study the behaviour of the total cross–section versus $\sqrt{s}$. Since a variety of SUSY particles are exchanged in the vertices and boxes, we expect that more threshold effects will appear. In Fig.4, we present the total cross–section against $\sqrt{s}$ in the MSSM case L (left curve) and MSSM case H (right curve) for several values of M_A. It can be seen from the plot that there is a peak in both cases. In the MSSM case L, the peak appears at $\sqrt{s} \approx 400$ GeV since in this case the masses of SUSY particles are approximately 200 GeV. In MSSM case H, the peak shows up for $\sqrt{s} \approx 1$ TeV. As one can see, the lighter M_A is, the more spectacular are the peaks. In the MSSM case L, for $\sqrt{s} < 1.2$ TeV the dominant contribution to the total cross–section is from vertex diagrams, while for energy $\sqrt{s} > 1.2$ TeV it is the box diagrams which dominate. Similarly in the MSSM case H, the vertex contibution dominates for $\sqrt{s} < 2.2$ TeV while the box diagram dominate if $\sqrt{s} > 2.2$ TeV.

4. Summary

We have computed the cross–section for the production mechanism $e^+e^- \to A^0Z$ at high energy e^+e^- colliders in the framework of the MSSM. Such a process proceeds via higher order diagrams and is strongly model dependent.

The calculation was performed within the dimensional regularisation scheme and we

presented results for both the MSSM and THDM. In the former case light SUSY particles may give important contributions to the cross–section, resulting in maximum values of order 0.003 fb. Therefore the SUSY enhancement is not sufficient to produce an observable signal at the planned luminosities of $500\,fb^{-1}$. In the MSSM with explicit CP violating phases, the pseudoscalar contains a CP even component and may be produced with an observable cross-section [32]. Therefore signals in the Higgsstrahlung channel for all h^0, H^0 and A^0 could not be explained in the MSSM unless SUSY sources of CP violation are present. Observation of this process might enable one to distinguish between SUSY and non–SUSY Higgs sectors. We showed that threshold effects may enhance the cross–section.

References

[1] S. Weinberg, Phys. Rev. Lett. **19** (1967) 1264; S. L. Glashow, Nucl. Phys. **22** (1961) 579. A. Salam, in *Elementary Particle Theory*, ed. N. Svartholm, (1968) 367.

[2] B. Pitrzyk, results presented at XXXth ICHEP, Osaka, Japan, July 27-August 2 (2000)

[3] R. Barate *et al.* [ALEPH Collaboration], Phys. Lett. B **495**, 1 (2000); M. Acciarri *et al.* [L3 Collaboration], Phys. Lett. B **495** (2000) 18;

[4] P. Abreu *et al.* [DELPHI Collaboration], Phys. Lett. B **499** (2001) 23; G. Abbiendi *et al.* [OPAL Collaboration], Phys. Lett. B **499**, 38 (2001)

[5] See for instance:
http://lephiggs.web.cern.ch/LEPHIGGS/papers/index.html

[6] M. Carena *et al.*, Report of the Tevatron Higgs Working Group, Fermilab-Conf-00/279-T, SCIPP 00/37, hep-ph/0010338. and refs therein.

[7] ATLAS Collaboration, Detector and Physics Performance Technical Design Report, http://atlasinfo.cern.ch/Atlas/GROUP/PHYSICS/TDR/access.html;

[8] J.F. Gunion, H.E. Haber, G.L. Kane and S. Dawson, *The Higgs Hunter's Guide* (Addison–Wesley, Reading, 1990).

[9] H. P. Nilles, Phys. Rept. **110** (1984) 1; H. E. Haber and G. L. Kane, Phys. Rept. **117** (1985) 75.

[10] H. Komatsu and J. Kubo, Phys. Lett. B **157**, 90 (1985). Nucl. Phys. **B 263** (1986) 265.

[11] K. Ackerstaff *et al.* [OPAL Collaboration], Eur. Phys. J. C **5**, 19 (1998); G. Abbiendi *et al.* [OPAL Collaboration], Eur. Phys. J. C **18**, 425 (2001); A. G. Akeroyd, J. Phys. G **G24**, 1983 (1998);

[12] M. Carena, S. Mrenna and C. E. Wagner, Phys. Rev. D **60**, 075010 (1999).

[13] T. Junk [LEP Collaborations], hep-ex/0101015.

[14] E. Accomando *et al.* [ECFA/DESY LC Physics Working Group Collaboration], Phys. Rept. **299**, 1 (1998).

[15] A. Djouadi, J. Kalinowski and P. M. Zerwas, Z. Phys. C **54**, 255 (1992).

[16] S. Dawson and L. Reina, Phys. Rev. D **60**, 015003 (1999).

[17] A. Djouadi, V. Driesen, W. Hollik and A. Kraft, Eur. Phys. J. C **1**, 163 (1998); M. Krawczyk, J. Zochowski and P. Mattig, Eur. Phys. J. C **8**, 495 (1999); A. Djouadi, V. Driesen, W. Hollik and J. Rosiek, Nucl. Phys. B **491**, 68 (1997).

[18] A. Arhrib, M. Capdequi Peyranere, W. Hollik and G. Moultaka, Nucl. Phys. B **581**, 34 (2000); S. Kanemura, Eur. Phys. J. C **17**, 473 (2000); S. H. Zhu, hep-ph/9901221.

[19] A. G. Akeroyd, A. Arhrib and M. Capdequi Peyranere, Mod. Phys. Lett. A **14**, 2093 (1999) [hep-ph/9907542].

[20] A. G. Akeroyd, A. Arhrib and C. Dove, Phys. Rev. D **61** (2000) 071702; A. G. Akeroyd and S. Baek, Phys. Lett. B **500**, 142 (2001) [hep-ph/0008286].

[21] G. J. Gounaris, P. I. Porfyriadis and F. M. Renard, hep-ph/0103135.

[22] G. 't Hooft and M. Veltman, Nucl. Phys. B **44**, 189 (1972). P. Breitenlohner and D. Maison, Commun. Math. Phys. **52** (1977) 11.

[23] A. Denner, H. Eck, O. Hahn and J. Kublbeck, Phys. Lett. B **291**, 278 (1992).

[24] See http://www.FeynArts.de.

[25] G. J. van Oldenborgh, Comput. Phys. Commun. **66**, 1 (1991).

[26] A. Dabelstein and W. Hollik, MPI-PH-93-86 *Contributed to Workshop on e+ e- Collisions at 500 GeV: the Physics Potential*; A. Dabelstein, Z. Phys. C **67**, 495 (1995) [hep-ph/9409375].

[27] J. F. Gunion and A. Turski, Phys. Rev. D **39**, 2701 (1989); Phys. Rev. D **40**, 2333 (1989). M. S. Berger, Phys. Rev. D **41** (1990) 225. Y. Okada, M. Yamaguchi and T. Yanagida, Prog. Theor. Phys. **85**, 1 (1991). H. E. Haber and R. Hempfling, Phys. Rev. Lett. **66**, 1815 (1991). J. Ellis, G. Ridolfi and F. Zwirner, Phys. Lett. B **257**, 83 (1991). R. Barbieri, M. Frigeni and F. Caravaglios, Phys. Lett. B **258**, 167 (1991). A. Yamada, Phys. Lett. B **263**, 233 (1991).

[28] B. Grzadkowski, J. F. Gunion and J. Kalinowski, Phys. Rev. D **60**, 075011 (1999).

[29] H. Baer, M. Brhlik, D. Castano and X. Tata, Phys. Rev. D **58**, 015007 (1998); M. Carena, D. Garcia, U. Nierste and C. E. Wagner, Phys. Lett. B **499**, 141 (2001);

[30] For a review see S. P. Martin and J. D. Wells, Phys. Rev. D **64**, 035003 (2001) [hep-ph/0103067]. and refs therein.

[31] K. Hagiwara and M. L. Stong, Z. Phys. C **62**, 99 (1994) [hep-ph/9309248]. V. Barger, K. Cheung, A. Djouadi, B. A. Kniehl and P. M. Zerwas, Phys. Rev. D **49**, 79 (1994) [hep-ph/9306270].

[32] M. Carena, J. R. Ellis, A. Pilaftsis and C. E. Wagner, Nucl. Phys. B **586**, 92 (2000) [arXiv:hep-ph/0003180]. A. G. Akeroyd and A. Arhrib, Phys. Rev. D **64**, 095018 (2001) [arXiv:hep-ph/0107040].